

Magnetic resonance imaging evaluation of the median nerve using histogram analysis in carpal tunnel syndrome

Murat Baykara¹, Tuba Tülay Koca², Adnan Demirel², Ejder Berk²

¹Department of Radiology, Kahramanmaraş Sütçü İmam University, School of Medicine, Kahramanmaraş, Turkey

²Department of Physical Medicine and Rehabilitation, Kahramanmaraş Sütçü İmam University, School of Medicine, Kahramanmaraş, Turkey

Abstract

Objective: Histogram analysis of digital images is a popular new tissue analysis method. It has recently attracted much attention, is used to describe prognostic biomarkers, to characterize tumors, and to assist a few applications that guide radiotherapy treatment. Here, magnetic resonance imaging (MRI) measurements of the median nerve in the carpal tunnel of patients with carpal tunnel syndrome (CTS) were analyzed.

Methods: Hospital records were scanned of the past 3 years and patients who were diagnosed as having CTS through clinical findings and electromyography (EMG) at our outpatient clinic were included retrospectively. Patients who were not diagnosed as having CTS with EMG and had MRI of the wrists were determined as the control group.

Results: A total of 96 wrist MRIs were studied, including 47 wrists with CTS (42 females, 5 males) and 49 normal wrists (39 females, 10 males). There was no significant difference between the groups in terms of sex ($p=0.188$), affected side ($p=0.065$), and age ($p=0.287$). The mean age of the entire patient group was 41.34 ± 13.14 years (range, 18-65 years). Entropy values of the CTS side were significantly lower than those of the normal side. Standard deviation and variances were also low. Histogram distribution parameters, skewness, and uniformity were statistically different as compared with the controls. No significant difference was observed among the other parameters.

Conclusion: Although the intensity of the median nerve in the carpal tunnel does not change in CTS, significant changes were observed in histogram analysis. These data may be helpful in making diagnoses and treatment decisions, and determining the disease severity in CTS in the future.

Keywords: Carpal tunnel syndrome, median nerve, histogram, magnetic resonance imaging

INTRODUCTION

Carpal tunnel syndrome (CTS) is the compression of the median nerve under the retinaculum when passing through the carpal tunnel. It is mostly a peripheral neuropathy originating from idiopathic causes (1, 2). In CTS, diagnosis consists of nerve conduction studies such as electromyography (EMG), which is the standard examination method together with clinical findings. Radiologic methods have been reported to be useful in diagnosis when there is a discrepancy between clinical findings and EMG. Magnetic resonance imaging (MRI) is used as a noninvasive method to demonstrate the carpal tunnel (3).

Histogram analysis of digital images is one of a new popular group of tissue analysis methods (4). This technique, which has recently attracted much attention, is used to describe prognostic biomarkers, to diagnose interstitial lung disease, to characterize tumors, and to assist a few applications that guide radiotherapy treatment (5-15).

In clinical practice, the images used for diagnostic purposes are digital. A two-dimensional digital image consists of small rectangular blocks or pixels (picture elements). Each of these is represented by a set of coordinates on the limb and each has a value that represents the gray-level intensity of that picture or volume item on the limb (5).

We can tie the concept of texture in a digital image according to the distribution of the gray level values between the pixels of a particular region of the image. The texture of the images shows the structure and arrangement of the

You may cite this article as: Baykara M, Koca TT, Demirel A, Berk E. Magnetic resonance imaging evaluation of the median nerve using histogram analysis in carpal tunnel syndrome. *Neurol Sci Neurophysiol* 2018; 35(3): 145-150.

Corresponding Author: Tuba Tülay Koca **E-mail:** tuba_baglan@yahoo.com **Submitted:** 05 May 2018 **Accepted:** 26 August 2018



OPEN ACCESS

parts of an object. Tissue analysis refers to various mathematical methods used to determine spatial variations in gray scale to obtain derivatives called 'texture properties,' which provide a measure of intra-lesional heterogeneity in the image. Tissue analysis is basically a technique that evaluates the signal properties, i.e., the location and density of pixels and the gray level intensity in digital images. Tissue properties are, in fact, mathematical parameters calculated from the pixel distribution that characterize the basic structure of the texture and hence the objects shown in the image (5).

Entropy is one of the parameters commonly used to measure parametric homogeneity in the region of interest (ROI) (16-19). It is a measure of gray level change in a histogram and is a parameter that shows the homogeneity in intensity (irregularity). When all data are the same, they are defined as zero and the number increases as the distribution becomes irregular (17, 19).

Uniformity refers to gray level distribution, which indicates how close the image is to having uniform distribution of gray shades, and as the number increases, the distribution becomes more uniform (17, 19). Skewness is a measure of symmetry, or more precisely, the lack of symmetry. A distribution, or data set, is symmetrical if it looks the same to the left and right of the center point. If there are more points to the left of the middle, it is positive and vice versa. Kurtosis is a measure of whether the data are heavy-tailed or light-tailed relative to normal distribution. That is, data sets with high kurtosis tend

to have heavy tails, or outliers. Data sets with low kurtosis tend to have light tails, or a lack of outliers. Uniform distribution would be the extreme case. If the histogram curve is a bell, its value is three, and if there is a sharper peak in the histogram, it is higher than three (19).

In this study, histogram analysis of MRI measurements of the median nerve in the carpal tunnel in patients with CTS were analyzed for the first time in the literature.

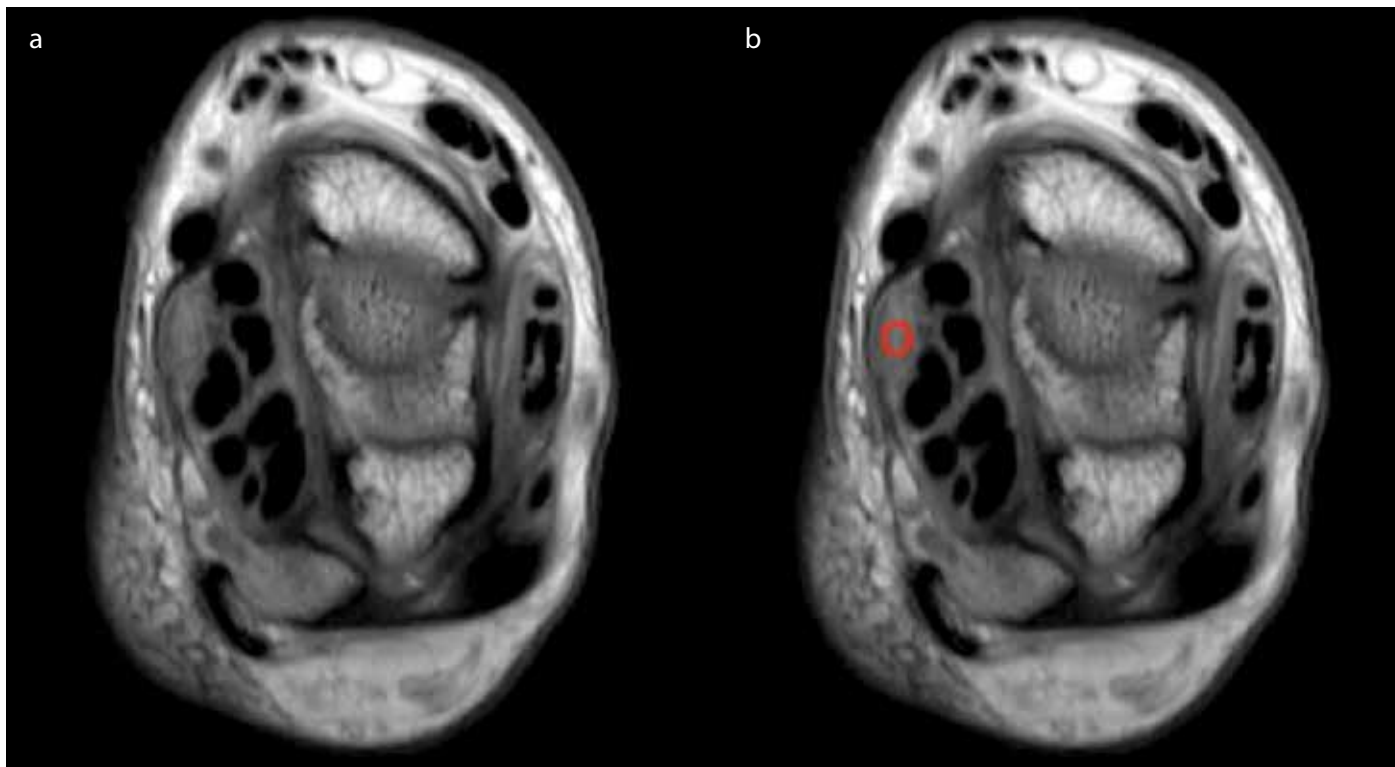
METHODS

We scanned our university hospital records of the past 3 years and patients who were diagnosed as having CTS through clinical findings and EMG at our outpatient clinic were included retrospectively. Patients who were not diagnosed as having CTS with EMG and had MRI (Philips Ingenia 1.5T; Philips, Holland) of wrists were determined as the control group. Patients with traumatic wrist injuries, a history of hand surgery, and inflammatory joint diseases that affected the wrists were excluded from the study. A scan reader radiologist was trained and totally blinded to the cases and the groups. Written informed consent form was taken from all participants. The study is complied with Helsinki declaration principles and no ethics committee approval was taken as it is designed as retrospectively.

Statistical Analysis

In proton density axial sections, the ROI of the portion of the median nerve corresponding to the center of the carpal

Figure 1. a, b. View of median nerve (a) and received ROI (b) in axial sections



tunnel was compared with each other (Figure 1). Histogram analysis from ROIs were performed using a (Matrix laboratory, MATLAB-based) computer program and compared using the Chi-square test and Student's t-test. Gray level intensity, standard deviation of histogram, entropy, uniformity, skewness, and kurtosis values were calculated from the ROI values. The entire image analysis algorithm was achieved by using an in-

house program (MATLAB, versionR2009b; MathWorks, Natick, Massachusetts, United States).

RESULTS

A total of 96 wrist MRIs were studied, including 47 wrists with CTS (42 females, 5 males) and 49 normal wrists (39 females, 10 males). There was no significant difference between the groups in terms of sex ($p=0.188$), affected side ($p=0.065$), and age ($p=0.287$) (Table 1).

The mean age of the entire study group was 41.34 ± 13.14 years (range, 18-65 years). Entropy values of the side with CTS were significantly lower than those of the normal side. Standard deviation and variances were also lower. Histogram distribution parameters, skewness, and uniformity parameters were statistically different as compared with the controls. No significant difference was observed between the other parameters (Table 2). The histogram analysis of the number and distribution of pixels in the MRIs of wrists with CTS and normal wrists were shown at Figure 2 and 3 respectively. There was no sign of CTS in the MRIs of the wrists with CTS.

DISCUSSION

The trapping of a peripheral nerve is caused by anatomical overtightening, which has become very narrow. This results in nerve damage and loss of function. In spite of their ubiqui-

Table 1. The distribution of sex of the participants included to the study

Sex			Normal, N	CTS, N	Total
Female	Side	Right	17	26	43
		Left	22	16	38
	Total		39	42	81
Male	Side	Right	4	3	7
		Left	6	2	8
	Total		10	5	15
Total	Side	Right	21	29	50
		Left	28	18	46
	Total		49	47	96

CTS: Carpal Tunnel Syndrome

Table 2. The analysis of histogram parameters of the normal and CTS side

	Normal		CTS			
	Mean	Std. Deviation	Mean	Std. Deviation		
Age	39.94	12.46	42.81	13.79	-1.071	0.287
Entropy*	4.87	0.37	4.53	0.39	4.444	0.000
Mean	97.25	20.03	95.51	18.57	0.440	0.661
Standard Deviation*	11.54	2.79	8.75	1.92	5.680	0.000
Minimum	67.65	25.11	74.79	19.07	-1.563	0.121
Maximum	121.88	21.55	118.68	21.12	0.734	0.465
Median	97.98	20.70	95.73	18.69	0.557	0.579
Variance*	140.92	69.04	80.27	34.72	5.402	0.000
Size%L	14.83	4.81	14.20	3.68	0.720	0.473
Size%U	15.34	3.33	16.23	3.08	-1.360	0.177
Size%M	69.82	7.23	69.57	4.74	0.207	0.837
Kurtosis	3.35	1.21	3.71	1.48	-1.329	0.187
Skewness*	-0.34	0.58	0.01	0.70	-2.680	0.009
Uniformity*	0.36	0.10	0.30	0.13	2.208	0.030

CTS: Carpal Tunnel Syndrome

*Statistically significant difference, $p < 0.005$

Figure 2. Histogram analysis of the number and distribution of pixels in the MRIs of wrists with CTS

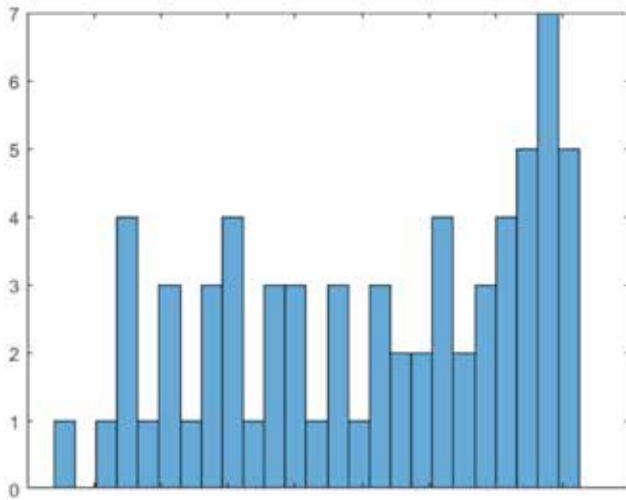
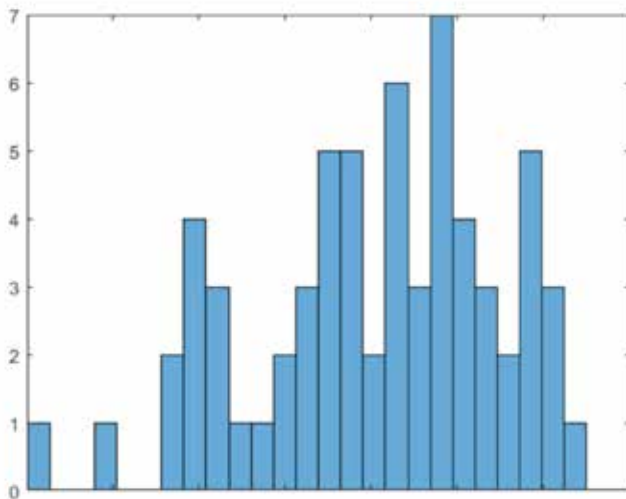


Figure 3. Histogram analysis of the number and distribution of pixels in the MRIs of normal wrists



tous nature, they are underdiagnosed, underreported, and sometimes not properly managed. Entrapment neuropathies are of various types, but the most common type is CTS. Clinical symptoms include pain, numbness and weakness in the hands and ankles (20, 21). Mechanisms involved in the pathophysiology of entrapment neuropathies include increased median nerve microcirculation damage, median nerve connective tissue and synovial tissue changes (22). Compression and stretching of the median nerve leads to impaired venous flow, edema and consequent mechanical and ischemic damage to the nerve. Nerve pressure and tension can cause damage to intraneural microcirculation, damage to the myelin sheath and axon, and changes in the surrounding connective and synovial tissue (23, 24).

Almost half of work-related injuries involve CTS, which result in interruptions to work (25). CTS is a disabling condition, even in its early stages, negatively affecting daily life and quality of life. Diagnostic tests such as MRI, ultrasound (USG), as well as provocative tests and nerve conduction studies, help to localize CTS diagnosis and nerve damage. Conservative methods should be applied in mild-to-moderate cases, whereas surgery is recommended for severe cases (26). Magnetic resonance imaging can show signal and configuration changes in the median nerve in patients with CTS. The increased signal in the thenar muscles indicates severe denervation, which can also be confirmed by EMG (27).

Clinical symptomatic CTS does not need to be supported by nerve conduction studies. Surgical decompression can provide complete relief from these symptoms. Decision of surgical decompression will be one of the issues discussed in the future because minimally invasive techniques have been able to reduce perioperative morbidity. For this reason new diagnostic tools are needed to make this decision. Diagnostic tools that provide dynamic recognition of CTS are also required (25, 28). Magnetic resonance imaging is accurate and reliable for the diagnosis and clinical follow up of these patients. It can help to avoid surgical decompression in patients with marked clinical symptoms and without measurable median nerve conduction disturbance (29).

In recent years, the role of MRI has also been related to the functional, metabolic, and cellular characterization of tissue morphologic imaging through advanced imaging techniques and the biologic behavior of the tissue. Today, 1.5 Tesla and more powerful MRI systems provide superior anatomic and morphologic imaging of pathologic tissues with high resolution (30). Digital interpretation of histogram data of MRI images of tissues has been the subject of research in many diseases and useful information about disease severity has been obtained. Goodyear et al. reported that skewness of fractional anisotropy could detect white matter damage associated with optic neuritis and its recovery (31). Yamashita et al. demonstrated that histogram analysis of computerized tomography (CT) images might be of clinical value in diagnosing otosclerosis (32). Colombi et al. analyzed changes over time in idiopathic pulmonary fibrosis (IPF) using a fully automatic histogram-based quantitative evaluation with CT (12).

According to our study, entropy, standard deviations, and variances were found lower on the side with CTS, indicating that the nerve had become more homogeneous. The change in the skewness indicates that the histogram returns to normal distribution and that the decline in uniformity appears to be a non-uniform distribution. The MRIs of median nerves in wrists with CTS differ from normal wrists in histogram analysis. We may say that the nerve becomes more homogeneous and uniform in CTS. In CTS, structural changes can be seen in

the median nerve due to microcirculation injury, and connective tissue and synovial tissue alterations.

There are limitations such as the fact that some patients had bilateral involvement, the number of male patients was not sufficient, and the signal intensity of ROIs has not yet been standardized. Additionally, we did not question the probable etiology of CTS, which could affect the median nerve structure and study results.

CONCLUSION

Although the intensity of the median nerve in the carpal tunnel does not change in CTS, significant changes are observed in histogram analysis. These data may be helpful in making diagnosis and treatment decisions, and determining the disease severity in CTS in the future.

Ethics Committee Approval: Authors declared that the research was conducted according to the principles of the World Medical Association Declaration of Helsinki "Ethical Principles for Medical Research Involving Human Subjects", (amended in October 2013).

Informed Consent: Written informed consent form was obtained from the patients who participated in this study.

Peer-review: Externally peer-reviewed.

Author Contributions: Concept - M.B., A.D.; Design -A.D., M.B.; Supervision - M.B.; Resources - A.D., E.B.; Materials - A.D., M.B.; Data Collection and/or Processing - A.D., M.B., E.B.; Analysis and/or Interpretation -T.T.K., M.B.; Literature Search - M.B., T.T.K.; Writing Manuscript M.B., T.T.K.; Critical Review -T.T.K.; Other - T.T.K.

Conflict of Interest: The authors have no conflicts of interest to declare.

Financial Disclosure: The authors declared that this study has received no financial support.

REFERENCES

1. Ibrahim I, Khan WS, Goddard N, Smitham P. Carpal tunnel syndrome: a review of the recent literature. *Open Orthop J* 2012; 6: 69-76. [\[CrossRef\]](#)
2. Amirfeyz R, Clark D, Parsons B, et al. Clinical tests for carpal tunnel syndrome in contemporary practice. *Arch Orthop Trauma Surg* 2011; 131: 471-474.
3. Ikeda M, Okada M, Toyama M, Uemura T, Takamatsu K, Nakamura H. Comparison of median nerve cross-sectional area on 3-T MRI in patients with carpal tunnel syndrome. *Orthopedics* 2017; 40: e77-e81. [\[CrossRef\]](#)
4. Park YW, Han K, Ahn SS, et al. Whole-tumor histogram and texture analyses of DTI for evaluation of IDH1-mutation and 1p/19q-codeletion status in world health organization grade II gliomas. *AJNR Am J Neuroradiol* 2018; 39: 693-698. [\[CrossRef\]](#)
5. Castellano G, Bonilha L, Li LM, Cendes F. Texture analysis of medical images. *Clin Radiol* 2004; 59: 1061-1069. [\[CrossRef\]](#)
6. Alic L, Niessen WJ, Veenland JF. Quantification of heterogeneity as a biomarker in tumor imaging: a systematic review. *PLoS One* 2014; 9: e110300. [\[CrossRef\]](#)
7. Chicklore S, Goh V, Siddique M, Roy A, Marsden PK, Cook GJ. Quantifying tumour heterogeneity in 18F-FDG PET/CT imaging by texture analysis. *Eur J Nucl Med Mol Imaging* 2013; 40: 133-140. [\[CrossRef\]](#)
8. Ganeshan B, Panayiotou E, Burnand K, Dizdarevic S, Miles K. Tumour heterogeneity in non-small cell lung carcinoma assessed by CT texture analysis: a potential marker of survival. *Eur Radiol* 2012; 22: 796-802. [\[CrossRef\]](#)
9. Yang D, Rao G, Martinez J, Veeraraghavan A, Rao A. Evaluation of tumor-derived MRI-texture features for discrimination of molecular subtypes and prediction of 12-month survival status in glioblastoma. *Med Phys* 2015; 42: 6725-6735. [\[CrossRef\]](#)
10. Tixier F, Hatt M, Le Rest CC, Le Pogam A, Corcos L, Visvikis D. Reproducibility of tumor uptake heterogeneity characterization through textural feature analysis in 18F-FDG PET. *J Nucl Med* 2012; 53: 693-700. [\[CrossRef\]](#)
11. Molina D, Perez-Beteta J, Luque B, et al. Tumour heterogeneity in glioblastoma assessed by MRI texture analysis: a potential marker of survival. *Br J Radiol* 2016:20160242.
12. Colombi D, Dinkel J, Weinheimer O, et al. Visual vs fully automatic histogram-based assessment of idiopathic pulmonary fibrosis (IPF) progression using sequential multidetector computed tomography (MDCT). *PLoS One* 2015; 10: e0130653. [\[CrossRef\]](#)
13. Ganeshan B, Abaleke S, Young RC, Chatwin CR, Miles KA. Texture analysis of non-small cell lung cancer on unenhanced computed tomography: initial evidence for a relationship with tumour glucose metabolism and stage. *Cancer Imaging* 2010; 10: 137-143. [\[CrossRef\]](#)
14. Aerts HJ, Bussink J, Oyen WJ, et al. Identification of residual metabolic-active areas within NSCLC tumours using a pre-radiotherapy FDG-PET-CT scan: a prospective validation. *Lung Cancer* 2012; 75: 73-76. [\[CrossRef\]](#)
15. Lambin P, Petit SF, Aerts HJ, et al. The ESTRO Breur Lecture 2009. From population to voxel-based radiotherapy: exploiting intra-tumour and intra-organ heterogeneity for advanced treatment of non-small cell lung cancer. *Radiother Oncol* 2010; 96: 145-152. [\[CrossRef\]](#)
16. Yu H, Caldwell C, Mah K, et al. Automated radiation targeting in head-and-neck cancer using region-based texture analysis of PET and CT images. *Int J Radiat Oncol Biol Phys* 2009; 75: 618-625. [\[CrossRef\]](#)
17. Ganeshan B, Miles KA, Young RC, Chatwin CR. Texture analysis in non-contrast enhanced CT: impact of malignancy on texture in apparently disease-free areas of the liver. *Eur J Radiol* 2009; 70: 101-110. [\[CrossRef\]](#)
18. Henderson S, Purdie C, Michie C, et al. Interim heterogeneity changes measured using entropy texture features on T2-weighted MRI at 3.0 T are associated with pathological response to neoadjuvant chemotherapy in primary breast cancer. *Eur Radiol* 2017; 27: 4602-4611. [\[CrossRef\]](#)
19. Suo ST, Zhuang ZG, Cao MQ, et al. Differentiation of pyogenic hepatic abscesses from malignant mimickers using multislice-based texture acquired from contrast-enhanced computed tomography. *Hepatobiliary Pancreat Dis Int* 2016; 15: 391-398. [\[CrossRef\]](#)

20. Wipperman J, Goerl K. Carpal tunnel syndrome: diagnosis and management. *Am Fam Physician* 2016; 94: 993-999.
21. Jiménez Del Barrio S, Bueno Gracia E, Hidalgo García C, et al. Conservative treatment in patients with mild to moderate carpal tunnel syndrome: A systematic review. *Neurologia* 2016 S0213-4853: 30094-30099.
22. Aboonq MS. Pathophysiology of carpal tunnel syndrome. *Neurosciences (Riyadh)* 2015; 20: 4-9.
23. Millesi H, Zöch G, Rath T. The gliding apparatus of peripheral nerve and its clinical significance. *Ann Chir Main Memb Super* 1990; 9: 87-97. [\[CrossRef\]](#)
24. Ozkul Y, Sabuncu T, Kocabey Y, Nazligul Y. Outcomes of carpal tunnel release in diabetic and non-diabetic patients. *Acta Neurol Scand* 2002; 106: 168-172. [\[CrossRef\]](#)
25. Wahab KW, Sanya EO, Adebayo PB, Babalola MO, Ibraheem HG. Carpal tunnel syndrome and other entrapment neuropathies. *Oman Med J* 2017; 32: 449-454. [\[CrossRef\]](#)
26. Britz GW, Haynor DR, Kuntz C, Goodkin R, Gitter A, Kliot M. Carpal tunnel syndrome: correlation of magnetic resonance imaging, clinical, electrodiagnostic, and intraoperative findings. *Neurosurgery* 1995; 37: 1097-1103. [\[CrossRef\]](#)
27. Horch RE, Allmann KH, Laubenberger J, Langer M, Stark GB. Median nerve compression can be detected by magnetic resonance imaging of the carpal tunnel. *Neurosurgery* 1997; 41: 76-82. [\[CrossRef\]](#)
28. Zamborsky R, Kokavec M, Simko L, Bohac M. Carpal tunnel syndrome: symptoms, causes and treatment options. Literature review. *Ortop Traumatol Rehabil* 2017; 19: 1-8. [\[CrossRef\]](#)
29. Somay G, Somay H, Cevik D, Sungur F, Berkman Z. The pressure angle of the median nerve as a new magnetic resonance imaging parameter for the evaluation of carpal tunnel. *Clin Neurol Neurosurg* 2009; 111: 28-33. [\[CrossRef\]](#)
30. Liu HS, Chiang SW, Chung HW, et al. Histogram analysis of T2*-based pharmacokinetic imaging in cerebral glioma grading. *Comput Methods Programs Biomed* 2018; 155: 19-27. [\[CrossRef\]](#)
31. Goodyear BG, Zayed NM, Cortese F, Trufyn J, Costello F. Skewness of fractional anisotropy detects decreased white matter integrity resulting from acute optic neuritis. *Invest Ophthalmol Vis Sci* 2015; 56: 7597-7603. [\[CrossRef\]](#)
32. Yamashita K, Yoshiura T, Hiwatashi A, et al. The radiological diagnosis of fenestral otosclerosis: the utility of histogram analysis using multidetectorrow CT. *Eur Arch Otorhinolaryngol* 2014; 271: 3277-3282. [\[CrossRef\]](#)